GEOLOGICA CARPATHICA, AUGUST 2005, 56, 4, 359–368

Mantle peridotite xenoliths in alkali basalts from the East Thrace region (NW Turkey)

FAHRİ ESENLİ and Ş. CAN GENÇ*

Istanbul Technical University, Department of Geological Engineering, 34469 Maslak, Istanbul, Turkey
*Corresponding author: scangenc@itu.edu.tr

(Manuscript received May 21, 2004; accepted in revised form March 17, 2005)

Abstract: This paper represents the first report on the peridotitic mantle xenoliths including spinel harzburgites and spinel lherzolites found in the Late Miocene-Pliocene basaltic rocks (Thracean alkaline basalts — TAB) of the Thrace region, northwestern Turkey. The lavas formed and extruded during the north-south extension of western Anatolia, are olivine basalts and basanites displaying within-plate affinity. The estimated modal mineralogy of the peridotite xenoliths is olivine (58–84 %) + orthopyroxene (12–35 %) + clinopyroxene (0–12 %) + spinel (1–5 %). They are characterized mainly by protogranular and also transitional protogranular to porphyroclastic and fine-grained equigranular textures. Melt pockets are recognized in only one sample. Deformation features in olivine and pyroxenes are zoning, twinning, including inclusions, kink banding, triple junction and undulatory extinction. Bulk-rock analyses indicate that the xenoliths are depleted in basaltic components (e.g. CaO — 0.39–1.50 wt. %, Al_2O_3 — 0.80–1.78 wt. %). Light rare-earth element (LREE) enrichment is significant (e.g. La_n 2–6), which suggests a cryptic metasomatic history.

Key words: Northwestern Turkey, geochemistry, petrology, mantle xenolith, alkali basalt, peridotite.

Introduction

Peridotite xenoliths in alkali basalts can be used as indicators of the composition of the upper mantle. The structures, textures, mineralogy, and chemical compositions of peridotite xenoliths provide information on the character of the lithospheric and/or astenospheric mantle (Frey & Green 1974; Nielson-Pike & Schwarzman 1977; Embey-Isztin et al. 1989). In this study, the peridotite xenoliths in two basalt eruptions from the Tekirdağ region (eastern Thrace, northwestern Turkey) were studied at Hacıköy (H) and Karatepe (K) (Fig. 1a–c). Eight xenoliths from Hacıköy and six xenoliths from the Karatepe eruptions were investigated petrographically. Moreover, three xenolith samples from Hacıköy and three from Karatepe were studied chemically. Xenoliths in alkali basalts from the Thrace were first reported by Esenli (1999), in which only the petrography and major element chemistry of the Hacıköy xenoliths were presented. In this study we present the major and trace elements, as well as REE data for the Hacıköy and Karatepe xenoliths and their petrologic and geochemical properties. In addition, the geochemical characteristics of the host basalts are treated and discussed briefly.

Geological setting

The mantle-derived xenolith-bearing basaltic lavas of Hacıköy and Karatepe are located in the Tertiary Thrace Sedimentary Basin, northwestern Turkey (Fig. 1a–c). The Thrace Basin is founded on the Intra-Pontide suture zone which was developed by the northward subduction of the northern branch of Neotethys Ocean during the Late Cretaceous–early Tertiary period (Şengör & Yılmaz 1981; Yılmaz et al. 1997) and continental collision of the Strandja and Sakarya Zones (Okay & Tüysüz 1999). The Thrace Basin started to open at the end of the Middle Eocene, and turned into a mature basin during the Oligocene time. In the center of the basin the thickness of the sedimentary rocks reaches up to 8 km (Turgut et al. 1991).

There are different views on the origin and the development mechanism of the Thrace Basin, as follows: **a** — it formed under the effects of a N–S directed extensional tectonic regime during the Middle Eocene to the latest Oligocene period after the closing of the Intra-Pontide Ocean (i.e. Turgut et al. 1991); **b** — it is a fore-arc basin formed during the Middle Eocene–Oligocene (i.e. Görür & Okay 1996); **c** — it is a ramp basin, which developed during the end of the Eocene–Oligocene period (i.e. Yılmaz et al. 1997; Yılmaz & Polat 1998) and **d** — it is a transtensional basin which is controlled by the Thrace-Eskişehir wrench fault (i.e. Yaltırak & Alpar 2002).

The young volcanic activity of the Thrace Basin occurred mainly in two major phases. The first phase formed during the Late Eocene–Early Miocene period which is assumed to be a product of Tibetan-type volcanism developed under the N-S compressional regime of northwestern Anatolia (i.e. Genç 1998; Yılmaz & Polat 1998). Calc-alkaline intermediate volcanic products alternating with the siliciclastics of the Thrace Basin extruded during this period. The second volcanic phase started during the Late Miocene (8–4 Ma), and produced distinctly different volcanic association. During this phase, the mantle-derived xenolith-bearing alkaline basaltic lavas extruded sporadically in different parts of the Thrace region (Fig. 1b,c).

The Thracean alkaline basalts (TAB) interfinger with the sediments of the Ergene Formation of the Late Miocene–

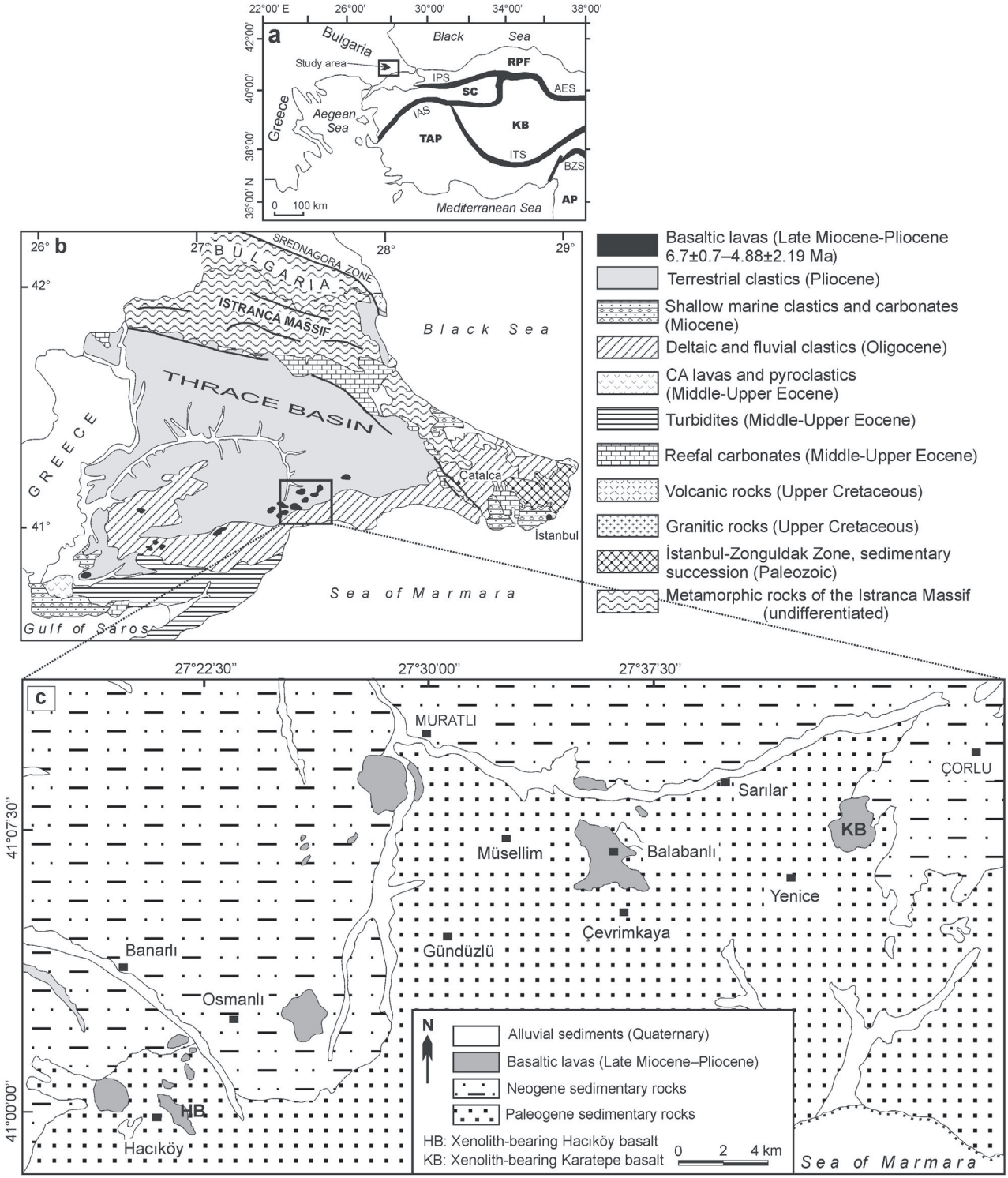

Fig. 1. Location map (**a**), simplified geological map of the Thrace region (**b**) (after Yılmaz et al. 1997), and the detailed geology map of the area studied (**c**) (compiled from Lebküchner 1974; Umut 1988a,b). Abbreviations for location map (a): **IPS** — Intra-Pontide Suture zone, **RPF** — Rhodope-Pontide Fragment, **SC** — Sakarya Continent, **IAS** — Izmir-Ankara Suture zone, **KB** — Kırşehir Block, **TAP** — Tauride-Anatolide Platform, **ITS** — Inner Tauride Suture zone, **BZS** — Bitlis-Zagros Suture zone, **AP** — Arabian Platform.

Pliocene consisting of the conglomerates, sandstones, siltstones and claystones. It unconformably overlies the older rock units of the region (Lebküchner 1974; Umut et al. 1983, 1984; Umut 1988a,b). The Quaternary alluvial deposits unconformably overlies the Thracean alkaline basalts represented by olivine basalt, basanite, trachybasalt lavas, and related pyroclastic rocks (Parejas 1939; Ternek 1949; Kopp et al. 1969; Lebküchner 1974; Ercan 1979; Umut et al.

1983, 1984; Sümengen et al. 1987; Ercan 1992; Yılmaz & Polat 1998; Esenli 1999). The K-Ar radiometric dating obtained from the TABs indicate the Late Miocene–Pliocene interval (6.7±0.7–4.88±2.19 Ma) (Sümengen et al. 1987; Yılmaz & Polat 1998 and the references therein).

It was proved that the Thracean alkaline basalts were formed under a N-S extensional tectonic regime, and thought to be extruded from the strike-slip fault zones cutting the entire Thrace lithosphere and the extensional cracks between the major fault zones (cf. Yaltırak 1996; Yılmaz & Polat 1998).

Analytical techniques

The host basalt lavas and the xenoliths were studied petrographically by polarizing microscope. The secondary minerals of the basalt lavas and some minerals of the xenoliths, particularly olivines were studied by X-ray powder diffraction analysis (XRD) method. For this purpose, the samples were ground and sieved to a grain size of 44 μm. A Philips diffractometer with CuKα radiation was used for X-ray analysis and holder samples were scanned at 1°2θ per minute. Xenolith and basalt samples were ground by agate mill for chemical analysis. Before these analyses, the rock specimens were crushed and xenoliths were separated from basalt. The thin outer rims of xenoliths were trimmed carefully from main bodies to make sure that the rest of the samples were pure xenolith. The chemical compositions of six xenolith and two basalt samples were analysed by using Spectro Ciros Vision ICP-ES for major oxides, Ba and Sc (0.200 g pulp sample by $LiBO_2$ fusion) and Cu, Zn and Ni (0.50 g sample leached with 3 ml 2–2–2 HCl–HNO_3–H_2O at 95 °C for one hour, diluted to 10 ml) and by Perkin Elmer Elan 6100 ICP-MS for the other elements in ACME Analytical Laboratories, Vancouver, Canada. A 0.2 g sample aliquot is weighed into a graphite crucible and mixed with 1.5 g of $LiBO_2$ flux. The flux/sample charge is heated in a muffle furnace for 15 minutes at 1050 °C. The molten mixture is removed and immediately poured into 100 ml of 5% HNO_3 (ACS grade nitric acid in de-mineralized water). The solution is shaken for 2 hours then an aliquot is poured into a polypropylene test tube. Calibration standards, verification standards and reagent blanks are added to the sample sequence.

Xenoliths

Petrography

The xenoliths are commonly rounded, subrounded, elliptical and rarely angular in shape. Their diameters vary from 0.5×0.5 to 5×7 cm, but most of them are 2×2 and 2×3 cm in size. They are yellowish-green and pale green in colour. The boundaries between xenoliths and host rock are clear and sharp, and there is not a transition zone between them on the specimens.

The xenoliths are commonly spinel harzburgite and rarely spinel lherzolite. Only two samples (HX4 and KX4) are classified as spinel lherzolite according to the IUGS systematics (Le Bas & Streckeisen 1991). Olivine-forsterite (58–84 %) + orthopyroxene-enstatite (12–35 %) + clinopyroxene-diopsite (0–12 %) + Cr-Spinel (1–5 %) assemblage is determined by using petrographic and XRD methods.

Texture features, rock type and estimated modal compositions (from the thin sections) of the Hacıköy and Karatepe xenoliths are given in Table 1. The texture of the xenoliths is commonly protogranular following the nomenclature of Mercier & Nicolas (1975). Considering the less common middle-grained crystals, it may be described as middle to coarse-grained texture (Fig. 2a,b). Elongated crystals together with the foliation and lineation are not recognized in the xenoliths. In some xenoliths, microcrystalline olivine and pyroxene aggregates are also recognized (Fig. 2c). Although these zones are similar to local transitions into the porphyroclastic texture, the typical porphyroclastic and equigranular textures are rare. In sample KX6, however, these aggregates are recognized as a crystallized melt pocket (Fig. 2e,h). In this melted area a smaller amount of plagioclase and serpentine occur among the olivine and pyroxene grains, but silica glass is not found. Spinel crystals are also present in this melted area (Fig. 2e), probably due to the interaction of the xenolith with the basaltic liquid (i.e. Bali et al. 2002). It is further supported that

Table 1: Petrographic features of the Thracean mantle xenoliths. **Ol** — olivine, **Opx** — orthopyroxene, **Cpx** — clinopyroxene, **Sp** — spinel.

Sample	Mineralogical composition				Rock	Texture
	Ol	Opx	Cpx	Sp		
HX1	70	25	×	5	Spinel harzburgite	Protogranular
HX2	74	22	×	4	Spinel harzburgite	Protogranular
HX3	84	15	×	1	Spinel harzburgite	Protogranular
HX4	58	25	12	5	Spinel lherzolite	Protogranular to porphyroclastic
HX5	71	20	7	2	Spinel harzburgite	Protogranular
HX6	84	12	2	2	Spinel harzburgite	Protogranular to fine-grained equigranular
HX7	79	20	×	1	Spinel harzburgite	Protogranular
HX8	82	14	2	2	Spinel harzburgite	Protogranular
KX1	64	35	×	1	Spinel harzburgite	Protogranular to fine-grained equigranular
KX2	61	30	8	1	Spinel lherzolite	Protogranular
KX3	84	15	×	1	Spinel harzburgite	Protogranular to porphyroclastic
KX4	71	15	12	2	Spinel lherzolite	Protogranular
KX5	69	30	×	1	Spinel harzburgite	Protogranular
KX6	72	25	×	3	Spinel harzburgite	Protogranular to fine-grained equigranular, with melt pockets

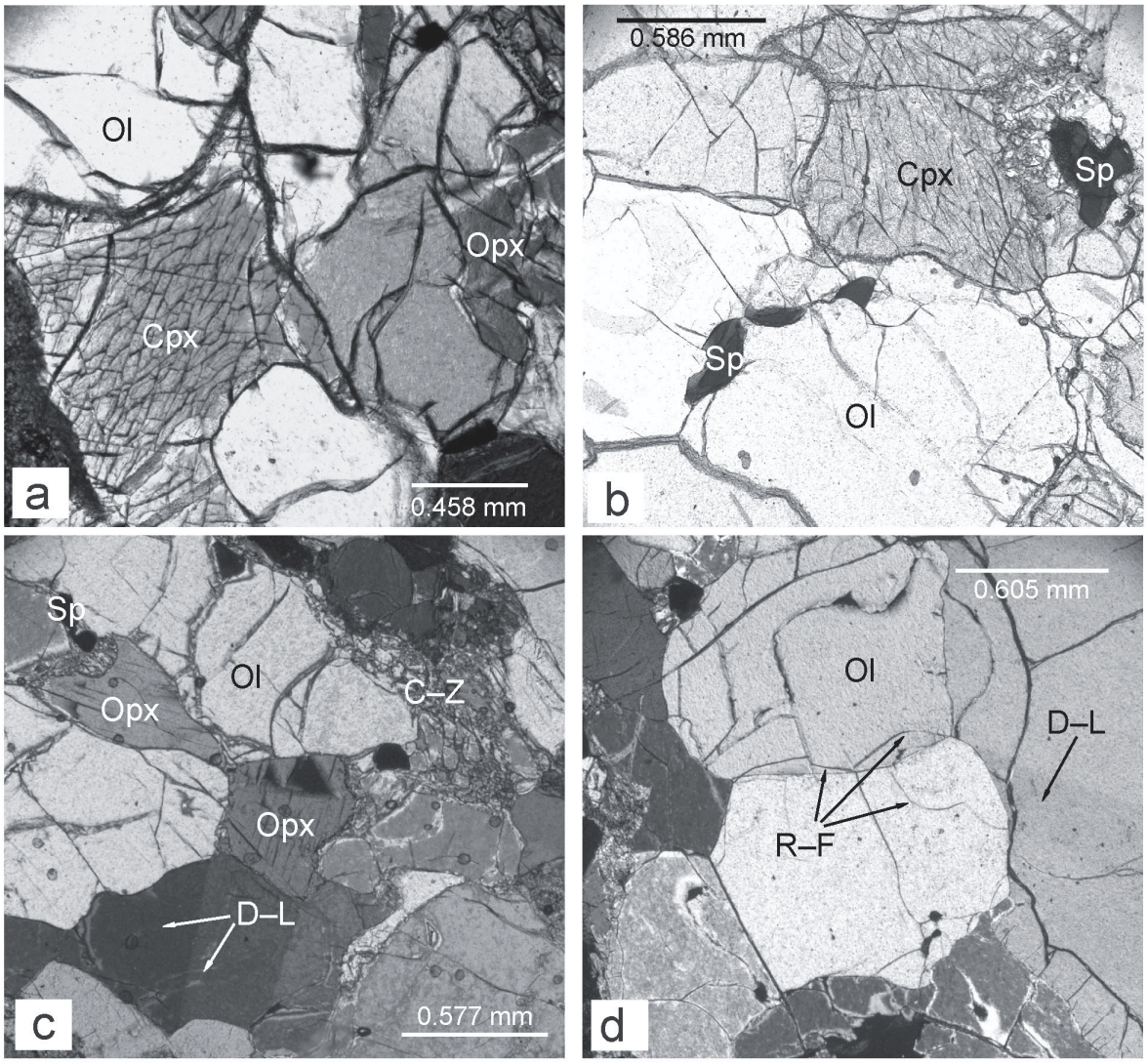

Fig. 2. Photomicrographs of the Thracean xenoliths. **a** — Spinel lherzolite xenolith with protogranular texture from the Hacıköy area (Ol — olivine, Opx — orthopyroxene, Cpx — clinopyroxene). **b** — Protogranular spinel lherzolite from the Karatepe area. On the upper right side of the photo, there is a melted and recrystallized area including the large spinel (Sp) crystal. **c** — Protogranular to porphyroclastic spinel harzburgite from the Karatepe area. The orthopyroxene displaying the deformation lamellae (D–L) and a crushed zone (C–Z) are also seen from the photo. **d** — The spinel harzburgite xenolith from the Karatepe area. The large olivines (Ol) display the rounded fracture patterns (R–F) and deformation lamellae (D–L).

brown transparent spinels are surrounded by an opaque rim in the samples of KX4 and KX6 (Fig. 2f). Some of the spinels are interstitial having holly leaf shape indicating the protogranular textures (Fig. 2g).

In all studied xenoliths, olivines are generally 0.5–3.0 mm in size and colourless or rarely pale green under the microscope. Large olivine grains have typically curvilinear boundaries in the Hacıköy xenoliths, whereas they have curvilinear and straight boundaries in the Karatepe xenoliths (Fig. 2d). The olivine was identified as forsterite by using XRD analysis. The d value of 222 spacing which is the distinguishable line among the four types of olivines was found to be 0.1749 nm. This spacing value confirms the forsterite (d: 0.1750 nm). Orthopyroxenes (enstatite) are optically colourless or pale green in colour and 0.5–1.0 mm in size (Fig. 2c). Clinopyroxenes (diopsite) were found in five samples (Table 1). Cr-spinels are anhedral in shape and their diameters are less than 0.5 mm (Fig. 2e,f,g).

Common characterictics of the Thracean xenoliths are zoning, inclusions and twinning, deformation lamellae, undulatory extinction, kink banding and triple junction (granoblastic-polygonal texture) in olivines and pyroxenes (Fig. 2c,d,g). Spongy and crushed zones around the pyroxenes and symplectic spinel-pyroxene coexistence is rarely recognized.

Geochemistry

The geochemical data for the Hacıköy and Karatepe xenoliths are presented in Table 2. The Hacıköy and Karatepe xenoliths are uniform with respect to their Al_2O_3 (0.80–

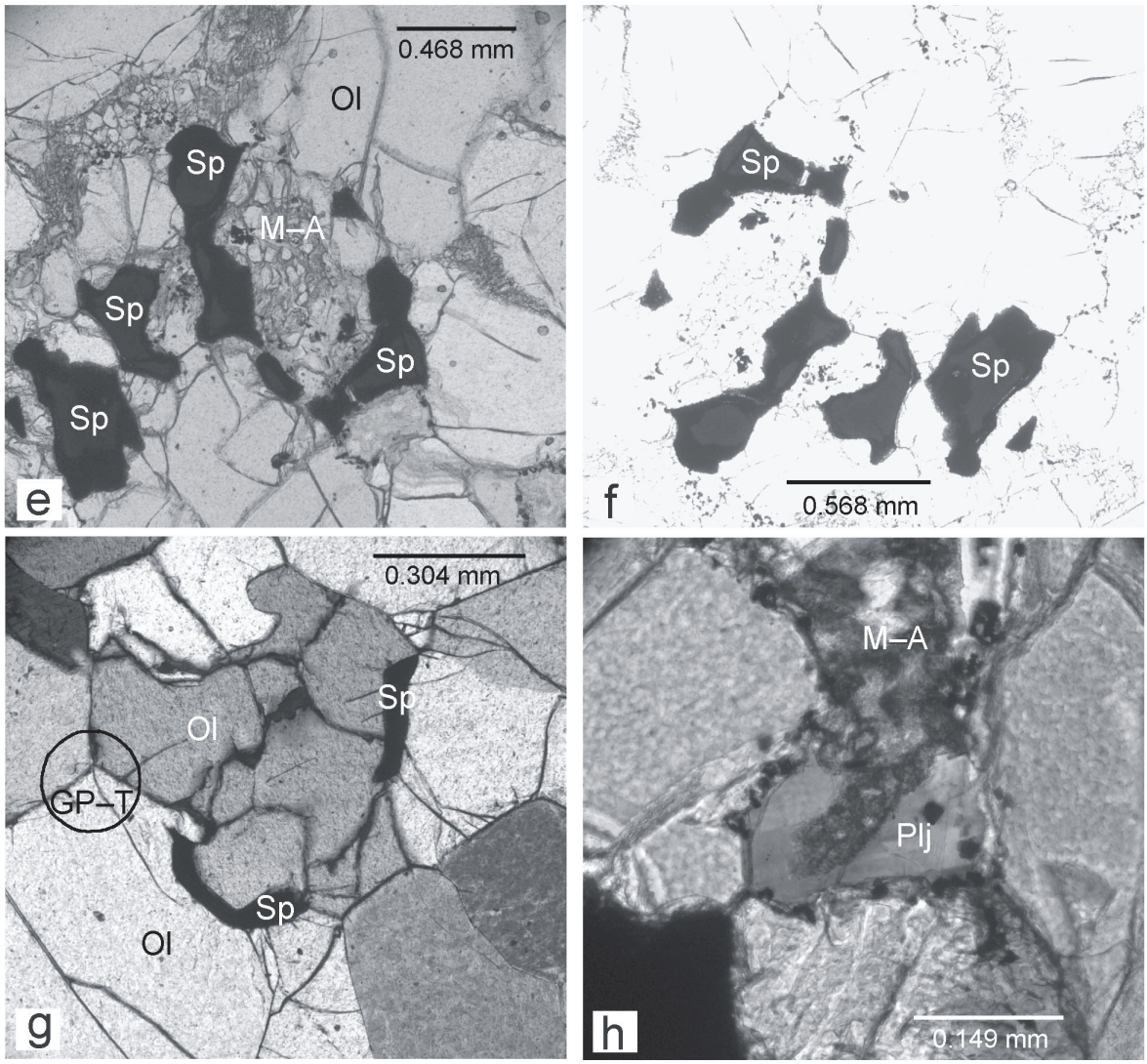

Fig. 2. ***Continued.*** **e** — Protogranular spinel harzburgite xenolith from the Karatepe area. The fine-grained melted-recrystallized area (M–A) and the large spinel (Sp) crystals embedded into this area. **f** — Spinel crystals with opaque rim and transparent core crystallized in the melted areas in the spinel harzburgite xenoliths from the Karatepe area. **g** — Protogranular and granoblastic-polygonal textures (GP–T) in the spinel lherzolite xenolith from the Karatepe area. Spinel crystals are interstitial with holly leaf shape indicative for the protogranular texture. **h** — The melt pocket bearing spinel lherzolite xenolith from the Karatepe area. A plagioclase crystal (Plj) crystallized in the melted/recrystallized area (M–A) is also seen.

1.78 wt. %) and MgO contents (43.89–47.26 wt. %). This situation appears to be in contrast with the peridotite xenoliths from other areas of the world (for example: the Pannonian Basin — Downes et al. 1992; west Hungary — Embey-Isztin et al. 1989; eastern China — Song & Frey 1989). All xenolith samples of the Hacıköy and Karatepe areas are highly depleted in "basaltic components". Therefore, the Al_2O_3 contents of the two locations vary from 0.80–0.84 wt. % to 1.68–1.78 wt. %, respectively (see Table 2). On the other hand, the CaO contents of the Hacıköy and Karatepe xenoliths range from 0.39–0.97 wt. % to 1.39–1.50 wt. % respectively. These CaO values imply that the Hacıköy xenoliths are extremely depleted (<1 wt. %), and the Karatepe xenoliths are strongly depleted (1–3 wt. %) xenoliths (cf. Wiechert et al. 1997). The Mg# of the two groups of xenoliths falls in a narrow range. The Mg# of the Hacıköy xenoliths is 0.91 and that of the Karatepe xenoliths is 0.90. The geochemical difference between the Hacıköy and Karatepe xenoliths may clearly be seen in their major element (i.e. TiO_2, Cr_2O_3, K_2O, Na_2O), trace element (e.g. Rb, Sr, Y), and the REE (La-Lu serie) contents (Table 2).

Use of MgO as a depletion/enrichment index for the mantle xenoliths is common. For this purpose, major and trace elements and REE of the xenoliths are plotted on the Harker-type diagrams versus MgO (Fig. 3). Ni, Cr, Co and Ga show a positive correlation, whereas SiO_2, Al_2O_3, TiO_2, CaO, $Fe_2O_3^t$, Na_2O, Sc, Y, V, and Lu display a negative correlation with MgO (Fig. 3).

The Hacıköy and Karatepe xenoliths are REE-depleted and when compared with the C1 chondrite (Sun & McDonough

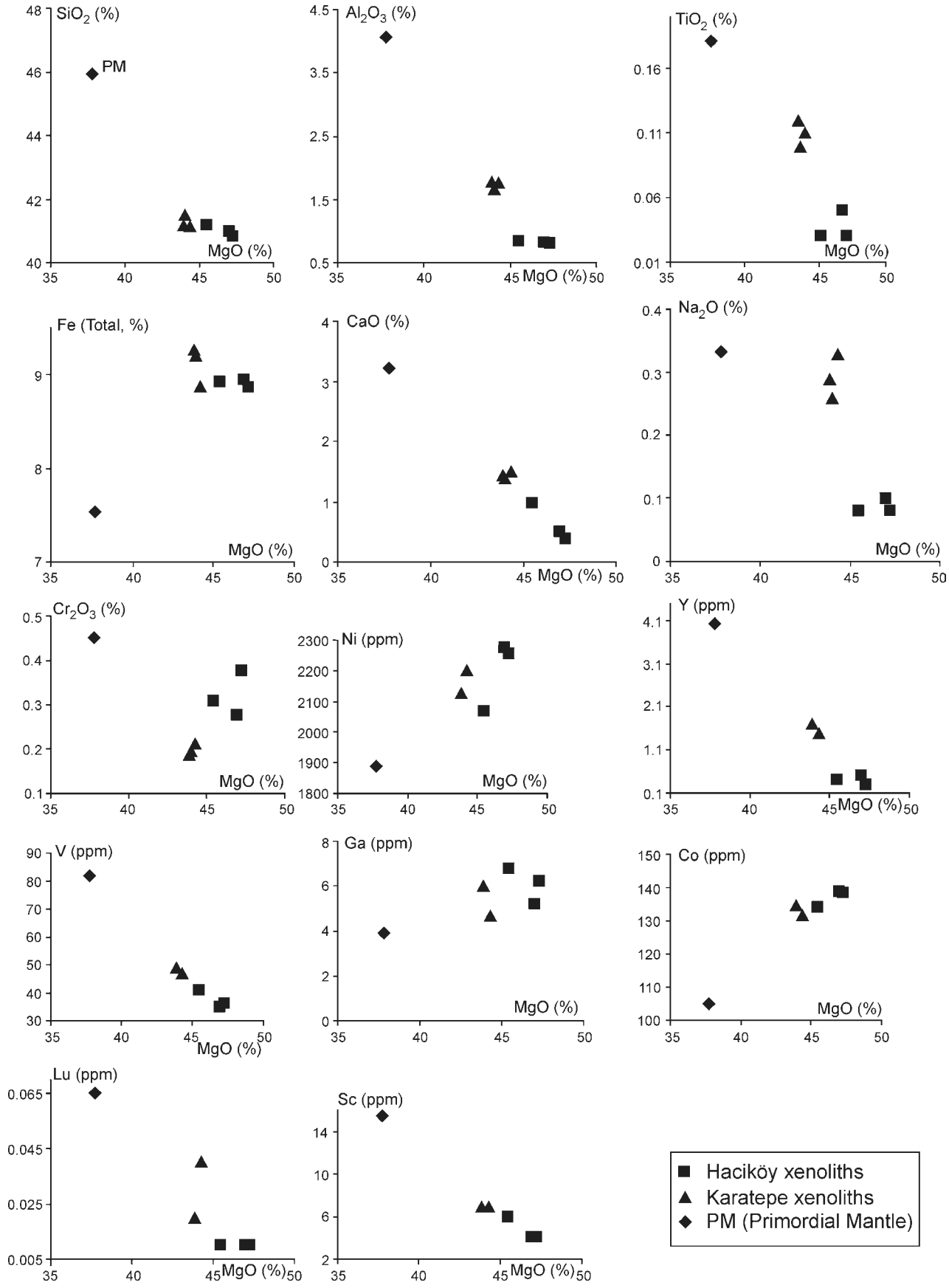

Fig. 3. The MgO versus major, trace and REE diagrams for the Thracean peridotite xenoliths.

Table 2: Geochemical data for the Hacıköy and Karatepe basalt lavas and related peridotite xenoliths (Mg# = Mg/(Mg+Fe); Fe_2O_3 is as total iron; n.d. = not determined).

	HB1 Host Basalt	KB1 Host Basalt	HX1 Xenolith	HX4 Xenolith	HX7 Xenolith	KX2 Xenolith	KX4 Xenolith	KX5 Xenolith
SiO_2	43.35	43.91	40.82	41.19	40.98	41.19	41.17	41.53
TiO_2	2.46	2.65	0.03	0.03	0.05	0.12	0.11	0.1
Al_2O_3	11.5	12	0.8	0.84	0.82	1.78	1.76	1.68
Fe_2O_3	11.16	11.13	8.85	8.91	8.94	9.26	8.87	9.21
MnO	0.17	0.16	0.12	0.12	0.12	0.13	0.13	0.12
MgO	14.19	11.95	47.26	45.47	46.97	43.89	44.3	44.01
CaO	8.51	8.85	0.39	0.97	0.5	1.44	1.5	1.39
Na_2O	3.43	3.57	0.08	0.08	0.1	0.29	0.33	0.26
K_2O	2.03	1.61	0.02	0.02	0.03	0.18	0.13	0.16
P_2O_5	0.84	0.72	0.07	0.06	0.06	0.08	0.07	0.07
Cr_2O_3	0.055	0.051	0.375	0.309	0.275	0.188	0.214	0.195
LOI	2.4	3	0.9	1.5	0.9	1.3	1.1	1.1
TOTAL	100.10	99.60	99.72	99.50	99.75	99.85	99.68	99.83
Mg#	0.72	0.68	0.91	0.91	0.91	0.90	0.90	0.90
Sc	17	18	4	6	4	7	7	
V	n.d.	182	36	41	35	49	47	
Co	28	55.6	138.2	133.7	138.6	134.5	131.6	
Ni	450	288	2255	2068	2275	2127	2202	
Cu	n.d.	51	27	16	25	30	28	
Zn	140	74	33	30	33	32	32	
Ga	n.d.	19.9	6.2	6.8	5.2	6	4.7	
Rb	28	19.4	0.8	1.3	1.3	4.6	3.4	
Sr	874	877	3	10.2	9.3	47.6	46	
Y	18	20.3	0.3	0.4	0.5	1.7	1.5	
Zr	192	234	3.2	3.5	4.9	11.3	10	
Nb	64	66	0.7	0.9	1.1	3	2.5	
Ba	440	342	5	5	5	23	19	
La	47	34	0.5	0.5	0.5	1.6	1.4	
Ce	76	66.6	0.5	0.6	0.9	3.1	2.5	
Pr	n.d.	8.37	0.06	0.16	0.14	0.4	0.33	
Nd	37	35.8	0.4	0.4	0.6	1.8	1.7	
Sm	7.2	7.1	0.1	0.1	0.1	0.3	0.4	
Eu	2.7	2.46	0.05	0.05	0.07	0.13	0.13	
Gd	n.d.	6.77	0.14	0.05	0.17	0.33	0.34	
Tb	0.5	0.92	0.01	0.01	0.01	0.05	0.05	
Dy	n.d.	4.9	0.06	0.09	0.1	0.34	0.28	
Ho	n.d.	0.88	0.05	0.05	0.05	0.07	0.06	
Er	n.d.	2.1	0.05	0.06	0.07	0.17	0.16	
Tm	n.d.	0.26	0.05	0.05	0.05	0.05	0.05	
Yb	1.6	1.6	0.08	0.05	0.15	0.24	0.22	
Lu	0.25	0.24	0.01	0.01	0.01	0.02	0.04	

1989), their (<10) × chondritic nature (Fig. 4) can clearly be seen. There is a considerable difference in REEs between the Hacıköy and Karatepe xenoliths. As seen on Figs. 4 and 5, the Karatepe xenoliths are more enriched in LREE, MREE and HREE compared to the Hacıköy xenoliths. The chondrite normalized patterns of xenoliths indicate that the Hacıköy samples are 0.2 to 2 × chondritic, while the Karatepe xenoliths are 0.5 to 8 × chondritic in nature (Fig. 4). The xenoliths display slightly concave-upward patterns (Fig. 4) in chondrite (C1)–normalized diagram. LREE enrichment is also evident from the ratios of $(La/Yb)_n$: (2.4–7.2) and (Sm/Nd): (0.51–0.76).

Host basalts

The Hacıköy and Karatepe basalts (TAB) are dark grey and black, massive, homogenous and locally fractured and slightly altered. Their textures are commonly microlitic. Although there are some differences between the Hacıköy and Karatepe lavas, the general mineralogical compositions and estimated mineral proportions are plagioclase (45–60 %) + olivine (10–14 %) + clinopyroxene (18–28 %) + orthopyroxene (3–8 %) + opaque (5–8 %) + amphibole (1–3 %) + secondary minerals in all studied basalt samples. They contain 15–30 % modal phenocrysts, among which pyroxene usually dominates. Groundmass consists mostly of microlites (plagioclase, pyroxene, and olivine) and a low percent of volcanic glass. Most of the olivines are represented by large phenocrysts. They are euhedral or subhedral in shape and rarely altered to iddingsite, carbonate and serpentine. Some of the olivines and orthopyroxenes in the Hacıköy and Karatepe basalts are probably xenocrysts derived from the xenoliths. Deformation features, such as strain lamellae, irregular extinction and kink banding are recognized in such olivine crystals. Clinopyroxene content ranges generally from 20 % to 25 % and most of them occur as microphenocrysts and microlites. Corona texture has formed around some pyroxene and olivine grains. In such grains the green outer zone and the pink inner zone can easily be identified. Plagioclases in the Karatepe basalts are larger (up to 0.5 mm) than the plagioclases in the Hacıköy basalts (< 0.1 mm). Opaque minerals are found as disseminated grains in the Hacıköy samples or zoned agglomerated crystals in the Karatepe samples and their content range up to 10 % in the Hacıköy samples.

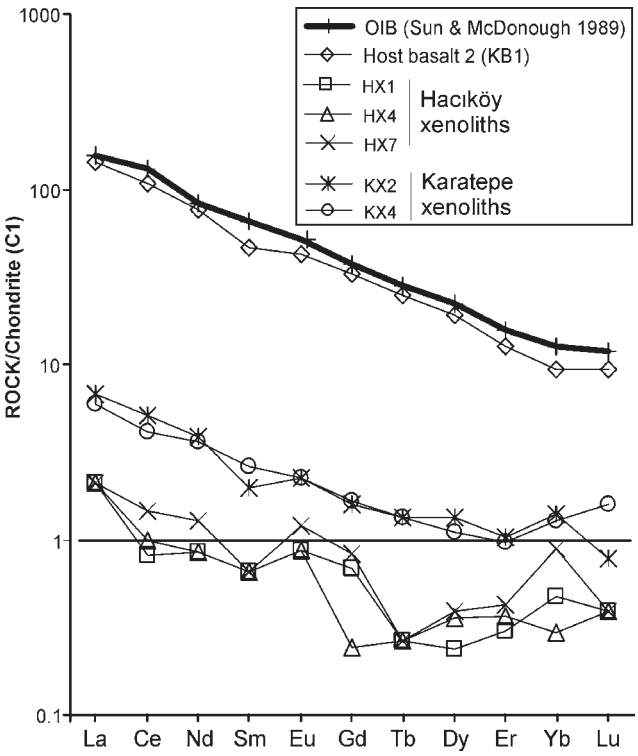

Fig. 4. Chondrite (C1)-normalized REE pattern for the Thracean peridotite xenoliths and host basalt lavas (normalization values are taken from Sun & McDonough 1989).

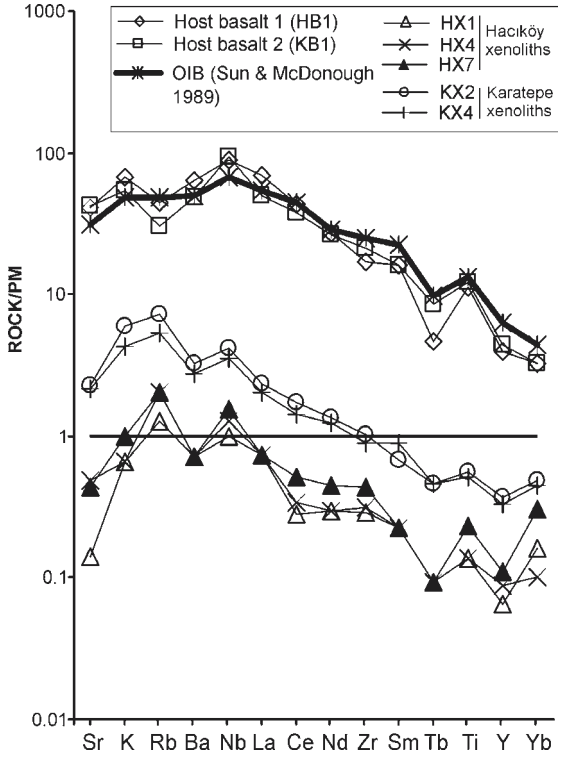

Fig. 5. Primordial mantle-normalized multi element variation diagram for the Thracean peridotite xenoliths and host basaltic lavas (normalization values are taken from Sun & McDonough 1989).

As the geochemical features of TABs were presented in detail in the previous works (i.e. Yılmaz & Polat 1998), their main characteristics are only presented briefly in the following paragraphs to avoid repetition. The two representative geochemical data for the Hacıköy and Karatepe basalts (samples HB1 and KB1) are given and pointed together with xenolith samples (see Table 2 and Figs. 4 and 5). The lavas display typical within plate alkaline (WPA) affinity. The evidence for this is as follows: **1** — curved convex patterns on spider diagrams, **2** — positive Nb anomaly, **3** — smoothly enriched REE patterns, **4** — relatively high contents of incompatible elements (for example Nb = 64–66 ppm, La = 34–47 ppm) and, **5** — high values of the ratios of Nb/La (1.3–1.9), Zr/Y (10.7–11.5) and Zr/Nb (3–3.5). These data are closely similar to WPA basalts reported from various regions of the world (Wood 1980; Sun & Mc Donough 1989).

In the Thrace region, the alkaline basaltic volcanism formed under the extensional tectonic regime and extruded along deep fracture zones, is characterized by a HIMU type OIB signature, and originated from the asthenospheric mantle source according to the Yılmaz & Polat (1998).

Discussion

According to the work of Mercier & Nicolas (1975), the xenoliths with protogranular texture are common in the European Tertiary and Quaternary volcanics, but the equigranular textured xenoliths are only present in the Quaternary volcanics. This conclusion is in good agreement with the case of the Thracean xenoliths. In the Thracean xenoliths, the sizes of olivine and pyroxene crystals are typically coarse. The other textural features of the Thracean xenoliths are as follows: in some xenoliths there are triple-junctions (granoblastic-polygonal texture) between the olivine and pyroxene crystals. Spongy and crushed zones around the pyroxenes and symplectic spinel-pyroxene coexistence are rarely recognized. The triple-junctions and rounded fracture patterns in the olivines suggest mantle deformation. Additionally, the curvilinear grain boundaries of olivine crystals and pyroxenes with spongy rims together with the crushed zones between the pyroxene and olivine crystals clearly indicate that the xenoliths are subjected to the partial melting at depths, and then recrystallized (Mercier & Nicolas 1974; Nielson Pike & Schwarzman 1977 and the references therein). It is evident from the melted area (recognized only in one sample) that the interactions between the basaltic liquids and xenoliths occurred (Embey-Isztin et al. 1989; Wiechert et al. 1997; Bali et al. 2002). Although the typical metamorphic textures such as foliation and lineation are not observed in the Thracean xenoliths, some undulatory extinction, deformation lamellae and the banding similar to twinning are the evidence for mantle deformations (Nielson Pike & Schwarzman 1977).

The Thracean xenoliths are the foreign fragments and do not represent the initial crystallization phases of basaltic liquids. The evidence for this may be given as follows: the compositions of the olivines, the deformation structures in the olivines and the pyroxenes, the triple-junctions and the granoblastic-

polygonal textures, and some textural features indicating the partial melting such as the spongy borders of pyroxenes and symplectic spinel-pyroxene growths, as mentioned above.

The decrease in SiO_2, TiO_2, Al_2O_3, CaO and Na_2O with the increase of MgO (Fig. 3) in the Thracean xenoliths indicates partial melting of original mantle material, and it is similar to the xenoliths reported in different areas of the world (i.e. Maaloe & Aoki 1977; Frey et al. 1985; Bodinier 1988; Embey-Isztin et al. 1989; Song & Frey 1989; Downes et al. 1992; Qi et al. 1995). All of the Thracean xenoliths cluster far from the primitive mantle composition (Fig. 3). The strong negative correlations of SiO_2, Al_2O_3 and CaO with MgO suggest considerable melt extraction from the original source, and its migration from the source region (c.f. Carter 1970; Kuno & Aoki 1970; Nickel & Green 1984; Downes 1987; Embey-Istzin et al. 1989). According to Frey et al. (1985), the negative variations of the moderately incompatible elements such as Sc, V and Y with MgO indicate that the amount of partial melting of the original source is less than 30 %. The positive correlation of Ni, and strong negative variations of Sc, V and Y with the MgO are in a good agreement with the spinel peridotitic mantle xenoliths examined by Jagoutz et al. (1979) and Jochum et al. (1989).

The La/Nb ratio for the Thracean xenoliths ranges from 0.45 to 0.71 which is 0.96 for the C1 chondrite (Sun & McDonough 1989). Generally, the upward-concave affinity of the REE patterns and the considerable LREE enrichment of the Thracean xenoliths (see Figs. 4 and 5) are in a good agreement with the metasomatically enriched mantle peridotites reported from the different regions of the world (e.g. O'Reilly & Griffin 1988; Zangana et al. 1998). This is supported by the ratio of $(La/Yb)_n > 1$. It is known that the values of $(La/Yb)_n$ of the mantle-derived xenoliths higher than one indicate the metasomatic enrichment (cf. Wiechert et al. 1997). On the other hand, occurrence of significant LREE enrichments and lack of H_2O-bearing phases such as amphibole and/or phlogopite in Thracean xenoliths indicates the xenoliths were affected by the cryptic metasomatism. The LREE depletion have already been reported from the typical mantle-derived peridotite xenoliths in numerous studies (e.g. Vaselli et al. 1995, and the references therein).

The LREE enrichment in the mantle xenoliths is commonly attributed to metasomatic fluids chromatographically percolated through upper mantle peridotite previously depleted in incompatible elements (e.g. Song & Frey 1989; Franz et al. 1997; Fodor et al. 2002). The LREE enrichment in the Thracean xenoliths may either be the result of subduction-related magmatism which occurred during the Late Cretaceous to early Tertiary period (Şengör & Yılmaz 1981; Yılmaz et al. 1997) or formed during the Upper Miocene–Pliocene extensional alkali basaltic volcanism. In the first case, the volatile and silica-rich melts could have been released from the subducted slab and could have caused the LREE enrichments above the subducting slab recorded in the Thracean mantle xenoliths similar to that of the Western Hungarian case (Bali et al. 2002).

The original depth of the Thracean xenoliths may be estimated from their mineralogical composition. According to the results of experimental petrology, the phase boundary between the spinel-peridotite and garnet-bearing peridotite is at ~1250 °C T and ~2–2.2 GPa P, corresponding to approximately 65 km of depth (e.g. O'Neill 1981; Qi et al. 1995; Shi et al. 1998; Klemme & O'Neill 2000; Fodor et al. 2002). Therefore, the lack of the garnet-peridotites in Thracean xenoliths constrains the maximum depth as 65 km.

Conclusions

The mantle-derived peridotite xenoliths occur in the Late Miocene–Quaternary Thracean alkaline basaltic suite. They display within plate alkaline affinity and are derived from the asthenospheric mantle reservoir. The xenoliths are sampled from two different localities, called Hacıköy and Karatepe, which are close to each other. The xenoliths are dominantly spinel-harzburgites, and less commonly spinel-lherzolites. These are thought to be the samples of the upper mantle beneath the Thrace region. The xenoliths are extremely and strongly depleted in basaltic components. The Thracean xenoliths are depleted in REE initially, and then enriched in LREE. The LREE enrichment either is probably a result of mantle metasomatism during the northward subduction of Neotethys ocean floor beneath the Pontides in the Late Cretaceous-early Tertiary period or due to the N-S directed extensional tectonic regime during which the alkaline basaltic volcanism were developed in the Late Miocene–Pliocene period.

Acknowledgments: The authors thank A. Okay, E. Demirbağ and O. Tüysüz who read and improved the text. Comments by C. Szabó and an anonymous reviewer are gratefully acknowledged.

References

Bali E., Szabó C., Vaselli O. & Török K. 2002: Significance of silicate melt pockets in upper mantle xenoliths from the Bakony-Balaton Highland volcanic field, Western Hungary. *Lithos* 61, 79–102.

Bodinier J.L. 1988: Geochemistry and petrogenesis of the Lanzo peridotite body, western Alps. *Tectonophysics* 149, 67–88.

Carter J.L. 1970: Mineralogy and chemistry of the Earth's upper mantle based on the partial fusion-partial crystallization model. *Geol. Soc. Amer. Bull.* 81, 2021–34.

Downes H. 1987: Relationship between geochemistry and textural type in spinel lherzolites, Massif Central and Languedoc, France. In: Nixon P.H. (Ed.): Mantle xenoliths. *John Wiley*, New York, 125–134.

Downes H., Embey-Isztin A. & Thirlwall M. 1992: Petrology and geochemistry of spinel peridotite xenoliths from the western Pannonian Basin (Hungary): evidence for an association between enrichment and texture in the upper mantle. *Contr. Mineral. Petrology* 109, 340–354.

Embey-Isztin A., Scharbert H.G., Dietrich H. & Poultidis H. 1989: Petrology and geochemistry of peridotite xenoliths in alkali basalts from the Transdanubian volcanic region, western Hungary. *J. Petrology* 30, 79–105.

Ercan T. 1979: Cenozoic volcanism in western Anatolia, Thrace and Eagean Island. *Jeoloji Mühendisliği Dergisi* 9, 23–46 (in Turkish with English abstract).

Ercan T. 1992: Cenozoic volcanism in Thrace and its regional distribution. *Jeoloji Mühendisliği Dergisi* 41, 37–50 (in Turkish with English abstract).

Esenli F. 1999: Peridotitic xenoliths in alkali basalts of Tekirdag re-

gion (Thrace). *Maden Tetkik Arama Enstitüsü Dergisi* 121, 125–139 (in Turkish with English abstract).

Fodor R.V., Sial A.N. & Gandhok G. 2002: Petrology of spinel peridotite xenoliths from northeastern Brazil: lithosphere with a high geothermal gradient imparted by Fernando de Noronha plume. *J. South Amer. Earth Sci.* 15, 199–214.

Franz L., Seifert W. & Kramer W. 1997: Thermal evolution of the mantle underneath the mid-German crystalline rise: evidence from mantle xenoliths from the Rhön area (Central Germany). *Contr. Mineral. Petrology* 61, 1–25.

Frey F.A. & Green D.H. 1974: The mineralogy, geochemistry and origin of lerzolite inclusions in Victorian basanites. *Geochim. Cosmochim. Acta* 38, 1023–1050.

Frey F.A., Suen C.J. & Stockman H.W. 1985: The Ronda high temperature peridotite: geochemistry and petrogenesis. *Geochim. Cosmochim. Acta* 49, 2469–2491.

Genç Ş.C. 1998: Evolution of the Bayramiç magmatic complex, northwestern Anatolia. *J. Volcanol. Geotherm. Res.* 85, 233–249.

Görür N. & Okay A.I. 1996: A fore-arc origin for the Thrace Basin, NW Turkey. *Geol. Rdsch.* 85, 662–668.

Jagoutz E., Palme H., Baddenhausen H., Blum K., Cendales M., Dreibus G., Spettel B., Lorenz V. & Wanke H. 1979: The abundances of major, minor and trace elements in the Earth's mantle as derived from primitive ultramafic nodules. In: R.B. Merrill (Ed.): Proceedings of the 10th Lunar and Planetary Science Conference. *Pergamon,* New York, 2031–2050.

Jochum K.P., McDonough W.F., Palme H. & Spettel B. 1989: Compositional constraints on the continental lithospheric mantle from trace elements in spinel peridotite xenoliths. *Nature* 340, 548–550.

Klemme S. & O'Neill H.S. 2000: The near-solidus transition from garnet lherzolite to spinel lherzolite. *Contr. Mineral. Petrology* 138, 237–248.

Kopp K.O., Pavoni N. & Schindler C. 1969: Geologie Thrakiens IV: Das Ergene Becken. *Beihefte Geol. Jb. Heft*. 76, 136.

Kuno H. & Aoki K. 1970: Chemistry of ultramafic nodules and their bearing on the origin of basaltic magmas. *Phys. Earth Planet. Inter*. 3, 273–301.

Le Bas M.J. & Streckeisen A.L. 1991: The IUGS systematics of igneous rocks. *J. Geol. Soc.* 148, 825–833.

Lebküchner R.F. 1974: Betrag zur kenntnis der geologie des Oligosans von mittel Thrakien (Türkei). *Bull. Miner. Res. Explor. Inst. Turkey* 83, 1–30.

Maaloe S. & Aoki K. 1977: The major element composition of the mantle estimated from the composition of lherzolites. *Contr. Mineral. Petrology* 63, 161–173.

Mercier J-C.C. & Nicolas A. 1975: Textures and fabrics of upper mantle peridotites as illustrated by xenoliths from basalts. *J. Petrology* 16, 454–487.

Nickel K.G. & Green D.H. 1984: The nature of the upper-most mantle beneath Victoria, Australia, as deduced from ultramafic xenoliths. In: Kornprobet J. (Ed.): Kimberlites. II. The mantle and crust-mantle relationships. *Elsevier,* Amsterdam, 161–178.

Nielson Pike J.E. & Schwarzman E.C. 1977: Classification of textures in ultramafic xenoliths. *J. Geol.* 85, 49–61.

Okay A.I. & Tüysüz O. 1999: Tethyan sutures of northern Turkey. In: Durand B., Jolivet L., Horvath F. & Seranne M. (Eds.): The Mediterranean Basins: Tertiary extension within the Alpine orogen. *Geol. Soc. London, Spec. Publ.* 156, 475–515.

O'Neill H.S. 1981: The transition between spinel lherzolite and garnet lherzolite, and its use as a geobarometer. *Contr. Mineral. Petrology* 77, 185–194.

O'Reilly S.Y. & Griffin W.L. 1988: Mantle metasomatism beneath western Victoria, Australia. I. Metasomatic processes in Cr-diopside lherzolites. *Geochim. Cosmochim. Acta* 52, 433–447.

Parejas E. 1939: Trakya linyitleri jeolojik etüdü, Uzunköprü, Keşan, Malkara, Hayrabolu mıntıkası. *MTA Rapor No. 981, Ankara* (unpublished report, in Turkish).

Qi Q., Taylor L.A. & Zhou X. 1995: Petrology and geochemistry of mantle peridotite xenoliths from SE China. *J. Petrology* 36, 55–75.

Shi L., Francis D., Ludden J., Frederiksen A. & Bostock M. 1998: Xenolith evidence for lithospheric melting above anomalously hot mantle under the northern Canadian Cordillera. *Contr. Mineral. Petrology* 131, 39–53.

Song Y. & Frey F.A. 1989: Geochemistry of peridotite xenoliths in basalt from Hannuoba, Eastern China: Implications for subcontinental mantle heterogeneity. *Geochim. Cosmochim. Acta* 53, 97–113.

Sun S.S. & McDonough W.F. 1989: Chemical and isotopic systematics of oceanic basalts: implications for mantle composition and processes. In: Saunders A.D. & Norry M.J. (Eds.): Magmatism in ocean basins. *Geol. Soc. Spec. Publ.* 42, 313–345.

Sümengen M., Terlemez İ., Sentürk K., Karaköse C., Erkan E.N., Ünay E., Gürbüz M. & Atalay Z. 1987: Stratigraphy, sedimentology and tectonics of the Gelibolu peninsula and SW Thracean Tertiary basin. *MTA Rapor No. 8128,* Ankara (unpublished report, in Turkish).

Şengör A.M.C. & Yılmaz Y. 1981: Tethyan evolution of Turkey: a plate tectonic approach. *Tectonophysics* 75, 181–241.

Ternek Z. 1949: Geological study of the region Kesan-Korudag. *Ph.D Thesis, Istanbul Univ*., Istanbul, 1–78.

Turgut S., Türkaslan M. & Perinçek D. 1991: Evolution of the Thrace sedimentary basin and its hydrocarbon prospectivity. *European Assoc. Petroleum Geoscientists Spec. Publ.* 1, 415–437.

Umut M. 1988a: Explanatory text for Kırklareli-C4 sheet. *MTA Genel Müdürlüğü 100,000 ölçekli açımsama nitelikli Türkiye Jeoloji Haritaları Serisi,* Ankara (in Turkish).

Umut M. 1988b: Explanatory text for Kırklareli-C5 sheet. *MTA Genel Müdürlüğü 1:100,000 ölçekli açımsama nitelikli Türkiye Jeoloji Haritaları Serisi,* Ankara (in Turkish).

Umut M., İmik M., Kurt Z., Özcan İ., Ateş M., Karabıyıkoğlu M. & Saraç G. 1984: Geology of the Edirne-Kırklareli-Lüleburgaz (Kırklareli)-Uzunköprü (Edirne) area and surroundings. *MTA Rapor No. 7604,* Ankara (unpublished report, in Turkish).

Umut M., Kurt Z. & İmik M. 1983: Geology of the Tekirdağ–Silivri (Istanbul)–Pınarhisar (Kırklareli) area and surroundings. *MTA Rapor No. 7349,* Ankara (unpublished report, in Turkish).

Vaselli O., Downes H., Thirlwall M., Dobosi G., Coradossi N., Seghedi I., Szakács A. & Vannucci R. 1995: Ultramafic xenoliths in Plio-Pleistocene alkali basalts from Eastern Transylvanian basin: depleted mantle enriched by vein metasomatism. *J. Petrology* 36, 1, 23–53.

Wiechert U., Ionov D.A. & Wedepohl K.H. 1997: Spinel peridotite xenoliths from the Atsagin-Dush volcano, Dariganga lava plateau, Mongolia: a record of partial melting and cryptic metasomatism in the upper mantle. *Contr. Mineral. Petrology* 126, 345–364.

Wood D.A. 1980: The application of Th-Hf-Ta diagram to problems of tectonomagmatic classification and to establishing the nature of crustal contamination of basaltic lavas of the British Tertiary volcanic province. *Earth Planet. Sci. Lett.* 50, 11–30.

Yaltırak C. 1996: Ganos fay sisteminin tektonik tarihi. *Türkiye Petrol. Jeol. Der. Bült*. 8–1, 137–150 (in Turkish with English abstract).

Yaltırak C. & Alpar B. 2002: Kinematics and evolution of the northern branch of the North Anatolian Fault (Ganos fault) between the Sea of Marmara and the Gulf of Saros. *Mar. Geol.* 190, 351–366.

Yılmaz Y., Tüysüz O., Yiğitbaş E., Genç Ş.C. & Şengör A.M.C. 1997: Geology and tectonic evolution of the Pontides. In: Robinson A.G. (Ed.): Regional and petroleum geology of the Black Sea and surrounding region. *AAPG Memoir* 68, 183–226.

Yılmaz Y. & Polat A. 1998: Geology and evolution of the Thrace volcanism, Turkey. *Acta Volcanol.* 10, 2, 293–303.

Zangana N.A., Downes H., Thirlwall M.F., Marriner G.F. & Bea F. 1998: Geochemical variation in peridotite xenoliths and their constituent clinopyroxenes from Ray Pic (French Massif Central): implications for the composition of the shallow lithospheric mantle. *Chem. Geol.* 153, 11–35.